

Single top quark production at the Tevatron

R. Schwienhorst^a

Michigan State University, 3234BPS, East Lansing, MI 48824, USA



The Tevatron experiments D0 and CDF have found evidence for single top quark production, based on datasets between 0.9 fb^{-1} and 2.2 fb^{-1} . Several different multivariate techniques are used to extract the single top quark signal out of the large backgrounds. The cross section measurements are also used to provide the first direct measurement of the CKM matrix element $|V_{tb}|$.

1 Introduction

Evidence for single top quark production at the Tevatron and a first direct measurement of the CKM matrix element $|V_{tb}|$ was first reported by the D0 collaboration¹. In contrast to top quark pair production through the strong interaction, which was observed in 1995^{2,3}, single top quarks are produced via the weak interaction. The Feynman diagrams for standard model (SM) s-channel (tb) and t-channel (tqb) single top quark production are shown in Fig. 1. There is third production mode, associated production of a top quark and a W boson, but its cross section is so small that it will not be considered further. The SM cross section for the s-channel process $p\bar{p} \rightarrow t\bar{b} + X, \bar{t}b + X$ is $0.88 \pm 0.14 \text{ pb}$ at NLO for $m_{\text{top}} = 175 \text{ GeV}$ ^{4,5}. At the same order and mass, the cross section for the t-channel process $p\bar{p} \rightarrow tq\bar{b} + X, \bar{t}q\bar{b} + X$ is $1.98 \pm 0.30 \text{ pb}$ ^{4,6}.

Measuring the single top quark production cross section provides a direct measurement of the CKM matrix element $|V_{tb}|$. The single top quark final state also allows for studies of the top quark polarization, and it is sensitive to many models of new physics, for example flavor changing neutral currents via the gluon⁷ or heavy new bosons W' that only couple to quarks⁸. The s-channel process is also an important background to Higgs searches in the associated production mode, and the advanced analysis techniques used in the single top searches will be applicable to Higgs searches as well.

^aOn behalf of the D0 and CDF collaborations.

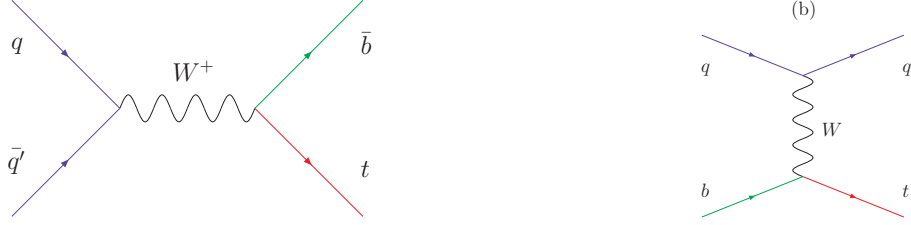


Figure 1: Feynman diagrams for s-channel (left) and t-channel (right) single top quark production at the Tevatron.

The D0 collaboration has updated two of their analysis methods using a dataset of 0.9 fb^{-1} . The updated results, including a combination of different methods are presented below. The CDF collaboration has analyzed a dataset of 2.2 fb^{-1} and significantly improved the sensitivity to single top quark production. These new results are presented below.

2 D0 results

2.1 Event selection

The D0 analysis selects electron+jets and muon+jets events in 0.9 fb^{-1} of data with the following requirements: One high- p_T lepton (electron ($p_T > 15 \text{ GeV}$) or muon ($p_T > 18 \text{ GeV}$)), missing transverse energy $\cancel{E}_T > 15 \text{ GeV}$, and between two and four jets with jet $p_T > 15 \text{ GeV}$ and jet 1 $p_T > 25 \text{ GeV}$, at least one is tagged with a neural-network based b-tagging algorithm. Additional cuts remove fake-lepton background events. Events are collected by lepton+jets trigger requirements.

The number of events observed in data and expected from the background model and SM signal is shown in Table 1. The largest sources of systematic uncertainty are the background normalization, jet energy scale, as well as b-tag and trigger modelling.

Table 1: Numbers of events expected by D0 in 0.9 fb^{-1} for electron and muon, 1 b -tag and 2 b -tag channels combined.

	2 jets	3 jets	4 jets
s-channel	16 ± 3	7 ± 2	2 ± 1
t-channel	20 ± 4	12 ± 3	4 ± 1
$t\bar{t}$	59 ± 14	134 ± 32	155 ± 36
W +jets	531 ± 129	248 ± 64	70 ± 20
Multijets	96 ± 19	77 ± 15	29 ± 6
Total background	686 ± 131	460 ± 75	253 ± 42
Data	697	455	246

Table 1 shows that after selection cuts, the expected SM single top signal is small compared to the background sum, and in fact the signal is significantly smaller than the background uncertainty. Thus, more advanced techniques are required to extract the signal.

2.2 Multivariate techniques

The D0 analysis employs three different multivariate techniques to extract the single top quark signal out of the large backgrounds. The boosted decision tree (BDT) analysis has not changed since the publication of evidence for single top quark production⁷. Here we focus on the Bayesian neural network analysis and the matrix element analysis, both of which have been re-optimized.

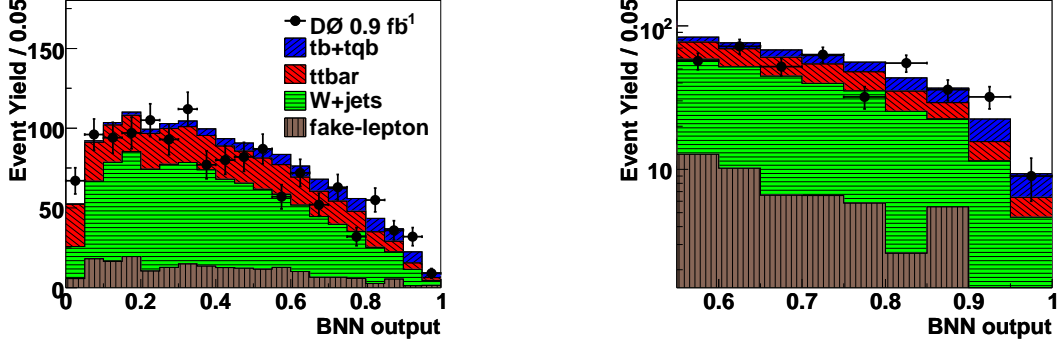


Figure 2: Comparison between data and background sum for the Bayesian neural network output. Shown is the full distribution (left), and the high-discriminant region (right). The signal has been normalized to the SM expectation.

In a conventional neural network, the network parameters and weights are determined in an optimization (training) procedure. Rather than optimizing for these network parameters once and then fixing them, the optimal network configuration can be obtained as an average over many different values for the network parameters. In this Bayesian procedure, an integration over all of the possible network parameter space is performed. The network architecture is fixed, and the weight of each set of parameters is obtained through a Bayesian integration. The final network discriminant is then the weighted average over all the individual networks. Fig. 2 shows the output of the BNN for the D0 data.

The Matrix element analysis starts from the Feynman diagrams for the single top quark processes and uses transfer functions to relate the parton level quark-level information to the reconstructed jet and other information. Matrix elements for the single top quark signal as well as the W +jets backgrounds are included. For 3-jet events, a top pair matrix element is also included. For each event, an integration over the phase space is performed, employing the transfer functions to compute the probability for this particular event to arise from a specific matrix element. A likelihood function is then formed as the ratio of the signal and signal plus background probabilities.

2.3 D0 summary

The cross section is measured as the peak of the Bayesian posterior probability density, shown in Fig. 3 for the ME analysis. The three different methods measure the following cross sections for the sum of s- and t-channel:

$$\begin{aligned}\sigma^{\text{obs}}(p\bar{p} \rightarrow tb + X, tqb + X) &= 4.9^{+1.4}_{-1.4} \text{ pb} \quad (\text{DT}) \\ &= 4.4^{+1.6}_{-1.4} \text{ pb} \quad (\text{BNN}) \\ &= 4.8^{+1.6}_{-1.4} \text{ pb} \quad (\text{ME}).\end{aligned}$$

The measured cross sections are consistent with each other and above the SM expectation.

The decision tree analysis has also measured the s- and t-channel cross sections separately,

$$\begin{aligned}\sigma^{\text{obs}}(p\bar{p} \rightarrow tb + X) &= 1.0 \pm 0.9 \text{ pb} \\ \sigma^{\text{obs}}(p\bar{p} \rightarrow tqb + X) &= 4.2^{+1.8}_{-1.4} \text{ pb},\end{aligned}$$

where the standard model cross section is used for the single top process not being measured.

Removing the constraint of the standard model ratio allows to form the posterior probability density as a function of both the tb and tqb cross sections. This model-independent posterior is shown in Fig. 3 (right) for the DT analysis, using the $tb+tb$ discriminant. The most probable value corresponds to cross sections of $\sigma(tb) = 0.9 \text{ pb}$ and $\sigma(tqb) = 3.8 \text{ pb}$. Also shown are

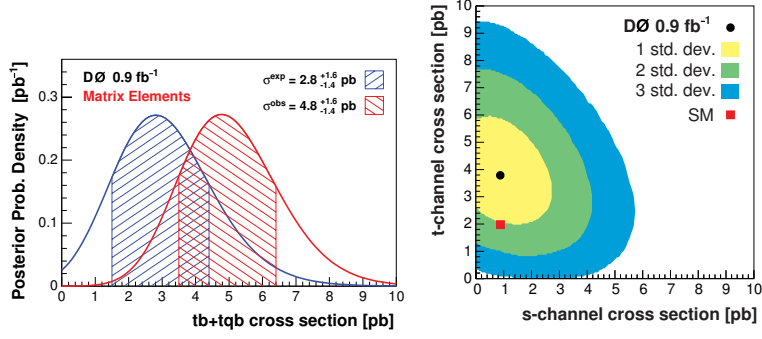


Figure 3: Posterior probability density for the matrix element analysis as a function of the sum of s-channel and t-channel cross sections (left), and for the BDT analysis as a function of both the s-channel and t-channel cross sections (right).

the one, two, and three standard deviation contours. While this result favors a higher value for the t -channel contribution than the SM expectation, the difference is not statistically significant. Several models of new physics that are also consistent with this result are shown in Ref.⁹. These updated results have recently been published¹⁰.

3 CDF results

3.1 Event selection

The CDF analysis selects electron+jets and muon+jets events in 2.2 fb^{-1} of data with the following requirements: One high- p_T lepton ($p_T > 20 \text{ GeV}$), $\cancel{E}_T > 25 \text{ GeV}$, and two or three jets with jet $p_T > 20 \text{ GeV}$, at least one of which is tagged by a displaced vertex tagging algorithm. Additional cuts remove fake-lepton background events. Events are collected by single-lepton trigger requirements. The matrix element analysis uses additional triggers in the muon channel to increase the acceptance.

The number of events observed in data and expected from the background model and SM signal is shown in Table 2. The largest sources of systematic uncertainty are the background normalization, jet energy scale, and b-tag modelling. Again, it is clear that a advanced analysis

Table 2: Numbers of events expected by CDF in 2.2 fb^{-1} for electron and muon, 1 b -tag and 2 b -tag channels combined.

	2 jets	3 jets
s-channel	41 ± 6	14 ± 2
t-channel	62 ± 9	18 ± 3
$t\bar{t}$	146 ± 21	339 ± 48
W +bottom	462 ± 139	141 ± 43
W +charm	395 ± 122	109 ± 34
W +light	340 ± 56	102 ± 17
Z +jets	27 ± 4	11 ± 2
diboson	63 ± 6	22 ± 2
Multijets	60 ± 24	21 ± 9
Total background	1492 ± 269	755 ± 91
Data	1535	752

techniques are required to extract the signal.

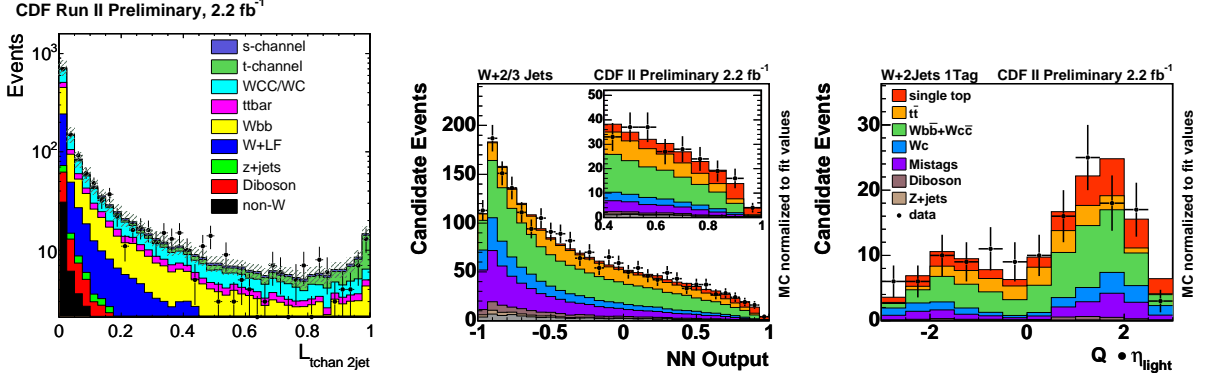


Figure 4: Comparison between data and background sum for the t-channel likelihood discriminant (left), the neural network discriminant (center), and the light quark jet pseudorapidity in the high-discriminant region for the neural network analysis (right). The signal has been normalized to the SM expectation.

3.2 CDF Likelihood Function

A multivariate likelihood is built from several kinematic variables that each separate the single top quark signal from the backgrounds. One special variable is a specially developed b-tagging neural network that aids in separating b-quark jets from light quark and c-quark jets. An additional special variable is a kinematic solver using constraints from the W boson mass and the top quark mass to determine if an event is well reconstructed. Another special variable is the t-channel matrix element, which uses the kinematic information provided by the kinematic solver. The likelihood discriminant for the t-channel likelihood is shown in Fig. 4 (left).

The measured cross section is obtained as the peak of a Bayesian posterior probability. The likelihood analysis measures a cross section of $\sigma(tb + tqb) = 1.8^{+0.9}_{-0.8}$ pb, below the SM expectation.

3.3 CDF Neural Network

Several kinematic variables as well as the b-tagging neural network output are combined in a neural network. Four different networks are built with 10-14 variables each, trained separately for 2-jet and 3-jet as well as 1-tag and 2-tag events. The full neural network output distribution is shown in Fig. 4 (center), and the signal region is shown in Fig. 4 (right). The neural network analysis measures a cross section of $\sigma(tb + tqb) = 2.0^{+0.9}_{-0.8}$ pb, below the SM expectation but consistent with the SM within uncertainties.

3.4 CDF Matrix Element

The matrix element analysis uses the same approach as described above, but also includes a top pair matrix element in the 2-jet bin. The matrix element for top quark pair events has more final state particles than the single top process, and these additional particles have to be integrated out. This is done by integrating over the kinematics of the hadronically decaying W -boson in a lepton+jets top pair event.

The Bayesian posterior probability density for the Matrix element analysis is shown in Fig. 5, showing the measured cross section and the measurement uncertainty. The measured cross section is $\sigma(tb + tqb) = 2.2^{+0.8}_{-0.7}$ pb, again below the SM expectation but consistent with the SM within uncertainties. The CKM matrix element $|V_{tb}|$ is also extracted from the posterior probability and a lower limit is found to be $|V_{tb}| > 0.59$ at the 95% confidence level.

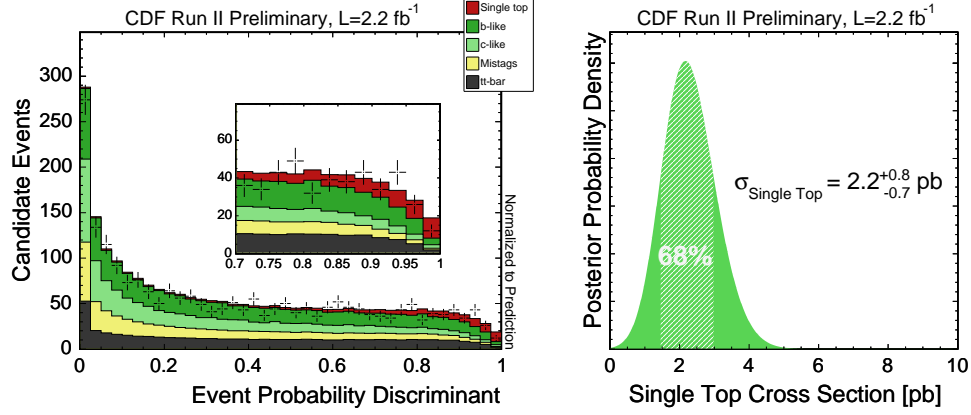


Figure 5: Data-background comparison for the matrix element discriminant (left) and Bayesian posterior density distribution observed by the Matrix element analysis.

4 Summary

Both Tevatron experiments have found better than 3 sigma evidence for single top quark production and have made the first direct measurement of the CKM matrix element $|V_{tb}|$ using advanced multivariate techniques. The CKM matrix element $|V_{tb}|$ can be measured to better than 15%. Further improvements to the analyses are in progress and both experiments are working towards observation of single top quark production at the 5 sigma level.

Acknowledgments

We thank the Fermilab staff and the technical staffs of the participating institutions for their vital contributions.

References

1. V.M. Abazov *et al.* (D0 Collaboration), Phys. Rev. Lett. **98**, 181802 (2007).
2. F. Abe *et al.* (CDF Collaboration), Phys. Rev. Lett. **74**, 2626 (1995).
3. S. Abachi *et al.* (D0 Collaboration), Phys. Rev. Lett. **74**, 2632 (1995).
4. Z. Sullivan, Phys. Rev. D **70**, 114012 (2004).
5. Q. H. Cao, R. Schwienhorst and C. P. Yuan, Phys. Rev. D **71**, 054023 (2005) [arXiv:hep-ph/0409040].
6. Q. H. Cao, R. Schwienhorst, J. A. Benitez, R. Brock and C. P. Yuan, Phys. Rev. D **72**, 094027 (2005) [arXiv:hep-ph/0504230].
7. V. M. Abazov *et al.* (D0 Collaboration), Phys. Rev. Lett. **99**, 191802 (2007) [arXiv:hep-ex/0702005].
8. V. M. Abazov *et al.* (D0 Collaboration), accepted by Phys. Rev. Lett, arXiv:0803.3256 [hep-ex].
9. T. Tait and C.P. Yuan, Phys. Rev. D **63**, 014018 (2001).
10. V. M. Abazov *et al.* (D0 Collaboration), accepted by Phys. Rev. D, arXiv:0803.0739 [hep-ex].